NJC

PAPER

View Article Online
View Journal | View Issue

Published on 14 October 2015. Downloaded by Michigan State University on 19/01/2016 18:25:29.

Cite this: *New J. Chem.*, 2015, 39, 9735

Self-assembly synthesis of Co_3O_4/multiwalled carbon nanotube composites: an efficient enzyme-free glucose sensor†

Raghavendra Prasad and Badekai Ramachandra Bhat*

Received (in Montpellier, France) 8th June 2015,
Accepted 29th September 2015

DOI: 10.1039/c5nj01447f

www.rsc.org/njc

Self-assembled cobalt oxide-multiwalled carbon nanotube composites were synthesized by simple and effective wet chemical routes. Using these materials, a modified glassy carbon electrode was fabricated and investigated for enzyme-free glucose sensor applications. The fabricated sensor exhibited a high sensitivity of 5089.1 μA mM^{-1} cm^{-2} with a detection limit of 10.42 μM over a glucose concentration ranging from 0.05 to 12 mM. The sensor also shows promising sensor features like stability, selectivity and fast detection. Moreover, the detection of glucose in human blood serum samples with the as-developed sensor agreed well with the results obtained from commercial glucose meters.

Introduction

Over the past two decades, major efforts have been devoted to the development of possible alternative materials for the electrochemical detection of glucose such as carbon nanotubes (CNTs), graphene, conducting polymers, *etc.*[1–3] Among carbon materials, CNTs are considered to be a potentially promising candidate because of their low cost, good conductivity, easily functionalized properties, large surface areas and excellent corrosion resistance in various electrolytes.[4,5] Ever since their discovery, because of the special structural, mechanical, electronic and fast electron transfer properties, CNTs have gained substantial attention in electronic applications.[6–8] Many researchers around the world have focused on the development of CNT decoration with metal and metal-oxide nanoparticles (NPs) to obtain the active components for non-enzymatic glucose sensors such as NiO, CuO, Co_3O_4, MnO_2, *etc.*[9–16] Generally these metal oxide based sensors directly electrooxidise the glucose mediated by M^{2+}/M^{3+} (M = metal) in alkaline medium. Taking the advantages of simplicity, reproducibility and stability in an aggressive environment, more and more attention has been paid to metal-oxide based non-enzymatic glucose sensing.[8–12] However, only a few studies have reported on glucose sensors based on Co_3O_4. Due to its low cost, high chemical stability and reasonably high specific capacitance, it has been widely studied and documented in energy and biosensor research, such as supercapacitors, biosensors and lithium-ion cathode materials.[17–22] As an important transition element, cobalt and its oxides have shown excellent sensing properties over a wide range of glucose concentrations.[13,14,19,20] However, due to the large surface area and greater ability to promote electron-transfer ability of the CNTs, composites of Co_3O_4 and MWCNTs are mainly used in sensor fabrication. Many methods have been reported for the synthesis of Co_3O_4–MWCNT nanocomposites.[17,23–26] However, these methods are associated with high cost, are complicated and uniform decoration of nanoparticles remains a great challenge. Therefore, a facile and cost-effective method for the large scale synthesis of uniformly decorated Co_3O_4–MWCNT composites is a challenge and a very active research area.

At the same time, diabetes is one of the major health concerns, which affects about 5% of the world's population,[27] hence continuous monitoring of the human blood sugar level has attained remarkable attention. However, glucose oxidase (GOx) enzyme based sensors play a leading role in blood sugar monitoring.[28–31] Even though the enzyme based sensor has good selectivity and high sensitivity, it is associated with the most common and serious limitations of environmental aspects such as temperature, humidity, pH and chemical reagents, resulting in damage to enzymes which leads to a lack of long-term stability.[32–34] To overcome these limitations, enzyme-free glucose sensors have been explored. The enzyme-free detection of glucose is associated with several advantages such as fabrication and storage conditions that are cheap and simple, no enzyme denaturation and degradation and the sensors have more stability towards higher temperatures, pH and more resistance to toxic chemicals which could reduce the working performance of enzyme-based glucose sensors.[35,36]

Herein, we report the self-assembled uniform decoration of Co_3O_4-NPs on the surface of MWCNTs by simple wet chemical routes. Poly(ethylene glycol) (PEG) was used as a

Department of Chemistry, National Institute of Technology Karnataka, Surathkal, Srinivasnagar-575025, India. E-mail: ram@nitk.edu.in, brchandra@gmail.com

† Electronic supplementary information (ESI) available. See DOI: 10.1039/c5nj01447f

Published on 14 October 2015. Downloaded by Michigan State University on 19/01/2016 18:25:29.

capping agent to control the Co_3O_4 size and an average diameter of 6.7 nm was achieved. Utilising the advantage of large surface area, the high electronic conductivity of the MWCNTs and the high catalytic activity of cobalt, the Co_3O_4–MWCNT composite samples are explored for possible electrochemical enzyme-free glucose sensor applications. The sensor parameters like optimised operating potential, sensitivity, limit of detection (LOD), selectivity and stability of the sensor were systematically investigated and compared with the reported nanomaterial based enzyme-free glucose sensors.

Experimental

Chemicals and reagents

Cobalt(II) acetate tetrahydrate, poly(ethylene glycol) 8000 (PEG) (M_w = 7000–9000), D-(+)-glucose, D-(−)-fructose, D-(+)-maltose monohydrate, sucrose, L-ascorbic acid (AA), uric acid (UA), dopamine hydrochloride (DA) and *N*,*N*-dimethylformamide (DMF) were obtained from Sigma-Aldrich and were used as received. All reagents were of analytical grade. All solutions were prepared using high quality deionized water (18.4 MΩ cm^{-1}). The human blood serum (HBS) samples were voluntarily given by patients for conducting the experiments and the study protocol was approved by the Institutional review board at National Institute of Technology, Karnataka. Patients gave voluntary written informed consent before their participation. The MWCNTs were synthesized, purified and functionalised using the reported procedure from our research group.[37] Briefly, MWCNT synthesis was carried out in a horizontal tubular furnace at atmospheric pressure. 300 mg of the nickel formate catalyst precursor with a $CaCO_3$ support was taken in a quartz boat, which was placed in the centre of the quartz tube. Initially argon gas was used to purge the reactor while the furnace was heated to 700 °C for 10 min. The CNTs were synthesized by passing the reaction mixture containing acetylene (20 standard cubic centimeters per minute (sccm)) and argon (200 sccm) gas in the ratio 1 : 10 for 15 min. After the growth the reaction chamber was cooled down slowly to room temperature and black amorphous carbon as a crude product was obtained. To purify the sample, the crude product was first heated under air atmosphere at 380 °C for 2 h to remove amorphous carbon and then stirred in dilute HCl to remove the catalyst and the $CaCO_3$ support. Finally, the sample was rinsed with distilled water to remove traces of acid.

Instruments

An Autolab PGSTAT30 (Eco Chemie) electrochemical workstation driven by NOVA 1.9 software was used to collect electrochemical data (www.metrohm-autolab.com). A conventional three-electrode cell assembly was used. The Co_3O_4–MWCNT nanocomposite modified glassy carbon electrode (GCE) was used as the working electrode. A standard calomel electrode and platinum wire were used as reference and counter electrodes, respectively. All the measurements were carried out at room temperature. The X-ray diffraction (XRD) patterns of the products were determined by a Philips X-ray diffractometer using Cu Kα radiation and Raman spectra were recorded at room temperature with a laser excitation wavelength of 532 nm. The morphologies of the nanostructures were observed by a JEOL JSM-6400F field emission scanning electron microscope (FESEM) and transmission electron microscopy (TEM) images were recorded using JEOL-3010F.

Preparation of Co_3O_4/MWCNT composites

The self-assembly uniform decoration of Co_3O_4 on the MWCNTs was achieved by a simple wet chemical method. The MWCNTs (20 mg), were taken in a solution of 20 mL of DMF consisting of cobalt(II) acetate tetrahydrate (10 mg) and PEG (10 mg). The weight ratio of the MWCNTs and the cobalt precursor was maintained to be 2 : 1 and PEG was used as a capping agent. The above suspension was ultrasonicated for 30 min for uniform dispersion and later further ultra-sonicated in a glycerol bath at 125 °C until the solution gets evaporated. The residue obtained was subjected to thermal treatment at 400 °C for 15 min under an ambient atmosphere. The product was collected as a black powder and stored for characterization and electrode fabrication. For comparison studies, pure Co_3O_4 was synthesized similarly.

Electrode fabrication

The GCE ($\varnothing$ = 4.0 mm) was polished using 0.3 μm and 0.05 μm alumina slurries, respectively to obtain a mirror-like surface and was then ultrasonically cleaned in ethanol and water successively. After these pre-treatments, the electrode was allowed to dry at room temperature. For the preparation of Co_3O_4/MWCNT modified electrodes, 5 mg of the Co_3O_4/MWCNT composite and 1 mL of 0.5 wt% Nafion solution were mixed ultrasonically. Then resulting suspensions (5.0 μL) were drop casted onto the GCE surface and allowed to dry prior to use. For comparison studies, the Co_3O_4/GCE and the MWCNT/GCE were prepared under identical conditions.

Results and discussion

Morphology and structural characterization

The Co_3O_4 NP decorated MWCNTs were prepared by the above mentioned wet-chemical method. The structure, morphology, and electrochemical properties towards direct glucose oxidation were examined. The cobalt is expected to electrocatalyse the glucose where the MWCNTs act as a transducer and provide fast electron movement and are expected to enhance the electronic signals.

The surface morphology of the synthesized Co_3O_4/MWCNT composite was characterized using FESEM and TEM analysis. An overview of the FESEM and TEM micrographs of the pure MWCNTs, Co_3O_4 and Co_3O_4/MWCNT composite are shown in Fig. 1a–e. The FESEM micrographs of the pure MWCNTs (Fig. 1a), appear like a mesh, on which Co_3O_4 NPs were decorated using the sol–gel method; these Co_3O_4-NPs are wrapped around the MWCNTs (Fig. 1b). Co_3O_4-NPs synthesized using a similar

 This journal is © The Royal Society of Chemistry and the Centre National de la Recherche Scientifique 2015

Published on 14 October 2015. Downloaded by Michigan State University on 19/01/2016 18:25:29.

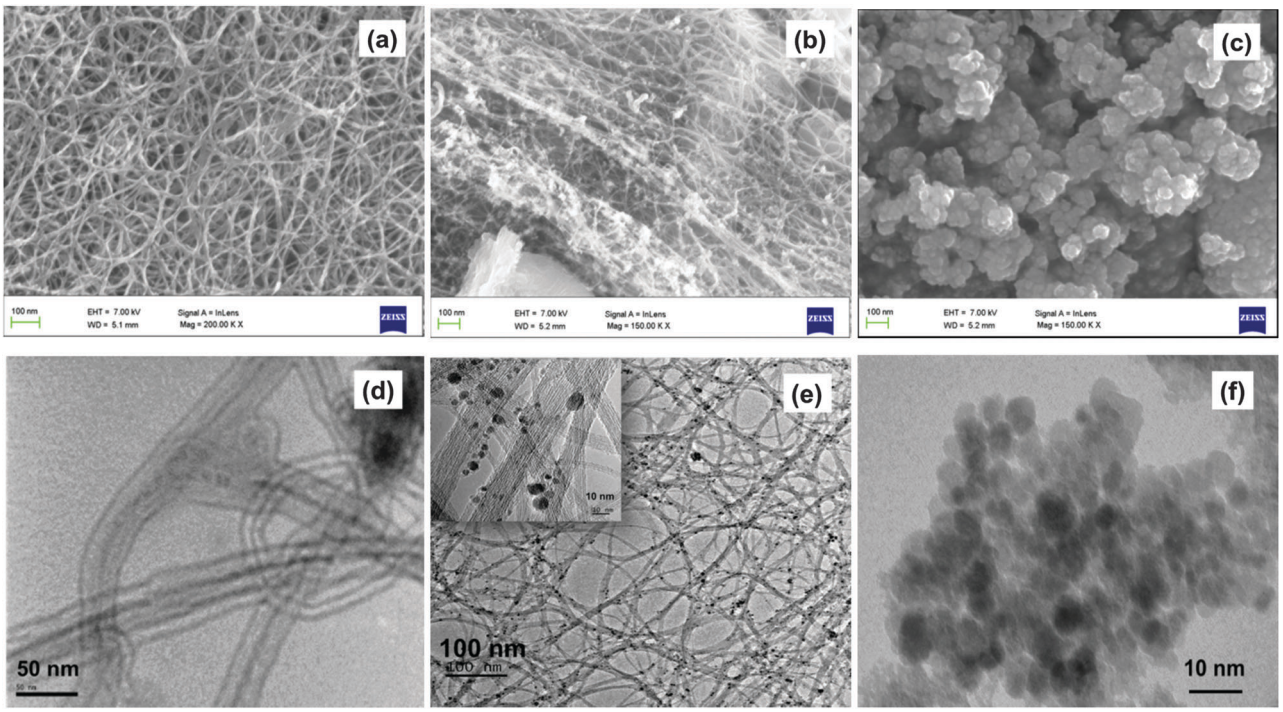

Fig. 1 FESEM images of (a) pure MWCNT, (b) Co_3O_4–MWCNT composite, (c) Co_3O_4 NPs and TEM images of (d) pure MWCNT, (e) Co_3O_4–MWCNT composite (with the higher magnification inset) and (f) Co_3O_4 NPs.

method appear to be granular particles in nature (Fig. 1c). The TEM micrograph of the MWCNTs (Fig. 1d) shows the average diameter of about 8.09 nm (Fig. S1a, ESI†) and a length of a few microns. However, in the composite sample, the TEM micrograph (Fig. 1e) shows an average size of about 2.9 nm (Fig. S1b, ESI†), dark spherical stain on the surface of the MWCNTs, which is attributed to the self-assembled Co_3O_4-NPs on the surface of the MWCNTs (Fig. S2, ESI†). The TEM micrograph of Co_3O_4-NPs synthesized appears to be granular in shape with an average size of about 6.7 nm (Fig. S1c, ESI†), which clearly suggested the formation of Co_3O_4-NPs. Hence, from the morphology studies it can be concluded that Co_3O_4-NPs were uniformly decorated on the surface of the MWCNTs.

The samples were further examined by XRD and the results are shown in Fig. 2a. These results exhibit different diffraction peaks associated with the MWCNTs and Co_3O_4. The diffraction pattern of the Co_3O_4–MWCNT shows the characteristic peaks of cubic Co_3O_4 and the peaks at 18.9°, 31.2°, 36.83°, 38.5°, 44.8°, 55.6°, 59.3° and 65.2° corresponding to (111), (220), (311), (222), (400), (422), (511) and (440) crystal planes (JCPDS no. 009-0148) along with the diffraction peak at 26.3° representing the (002) crystal plane of MWCNTs. However, a decrease in the relative intensity of the Co_3O_4 diffraction peaks in the composite sample is due to the amorphous nature of the MWCNTs. These results suggest that the obtained product by the sol–gel self-assembly process is a mixture of Co_3O_4 and MWCNTs and there were no other peaks in the spectrum indicating the high purity of the sample. The Raman spectra of the Co_3O_4–MWCNT hybrid were examined for further evidence of the successful assembly of Co on the MWCNTs. Fig. 2b shows the Raman

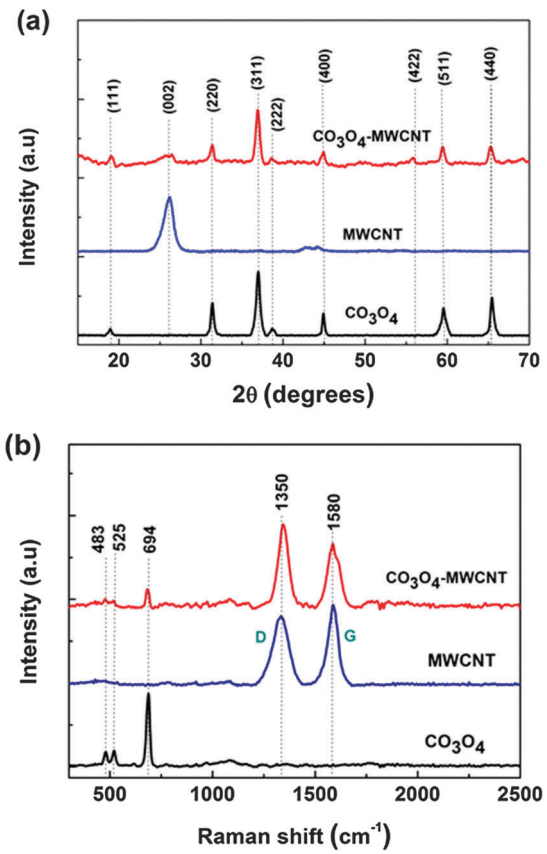

Fig. 2 (a) XRD spectra and (b) Raman spectra of Co_3O_4 NPs, pure MWCNTs and Co_3O_4/MWCNT nanocomposites.

Published on 14 October 2015. Downloaded by Michigan State University on 19/01/2016 18:25:29.

spectra of the synthesized samples. The peaks at $\sim$1337 cm^{-1} and $\sim$1586 cm^{-1} are the two characteristic peaks for the MWCNTs. The former is the D band which is ascribed to the glassy carbon or disordered graphite and the latter G-band corresponds to the vibrations of sp^2 bonded carbon atoms of the two-dimensional hexagonal lattice in graphite.[37,38] The I_D/I_G ratio was effectively used to evaluate the degree of disorder in the sample; increase in the I_D/I_G ratio from 0.81 to 1.21 for the MWCNTs and Co_3O_4–MWCNT was observed, which suggests that defects were introduced in the composite sample due to the destructive interaction of Co with the MWCNTs. In fact, the composite spectrum also shows three other peaks at 483 cm^{-1}, 525 cm^{-1} and 694 cm^{-1} which are attributed to Co_3O_4 which matches well with the spectrum recorded for pure Co_3O_4.[39,40]

Electrochemical behaviour of the Co_3O_4/MWCNT/GCE

The CVs of the Co_3O_4/GCE and Co_3O_4/MWCNT/GCE composite samples were investigated for the direct oxidation of glucose in both alkaline solution (0.2 M NaOH) and neutral phosphate buffer solution (0.1 M, pH 7.0) in the range from −0.4 V to 0.7 V (Fig. 3a). There was no oxidation or reduction peak seen in the phosphate buffer solution (inset Fig. 3a), while two pairs of well-defined redox peaks were obtained in NaOH solution. This redox peaks formed suggest that OH^- participates in the electrochemical redox reaction of Co_3O_4. From Fig. 3b, it is shown that the labelled pair of redox peaks I/II can be ascribed to the reversible transformation between Co_3O_4 and CoOOH while another pair of redox peaks III/IV can be assigned to further transition between CoOOH and CoO_2.[13,14,20] These two reversible redox reactions can be illustrated as in eqn (1) and (2):

$$Co_3O_4 + OH^- + H_2O \rightleftharpoons 3CoOOH + e^- \quad (1)$$

$$CoOOH + OH^- \rightleftharpoons CoO_2 + H_2O + e^- \quad (2)$$

The direct catalytic oxidation of glucose at the Co_3O_4/GCE and the Co_3O_4/MWCNT/GCE was first examined in 0.2 M NaOH. Fig. 3b presents the CVs in the absence and presence of 2 mM glucose of Co_3O_4/GCE (curve a and c) and Co_3O_4/MWCNT/GCE (curves b and d), respectively. Co_3O_4/GCE and Co_3O_4/MWCNT/GCE exhibited an oxidation peak for glucose starting at +0.25 and +0.20 V, respectively and covering the potential region where CoOOH and CoO_2 are formed. These results suggest that the direct catalytic oxidation of glucose in 0.2 M NaOH solution was due to CoOOH and CoO_2. From Fig. 3b it is also observed that with the addition of glucose, the Co_3O_4–MWCNT/GCE shows a notable increase in the redox peak current but a negligible increase in the case of the Co_3O_4/GCE, which can be attributed to the synergistic effect of Co_3O_4 and the MWCNTs making the substrate a better platform for electron transfer between Co_3O_4 NPs and the GCE.

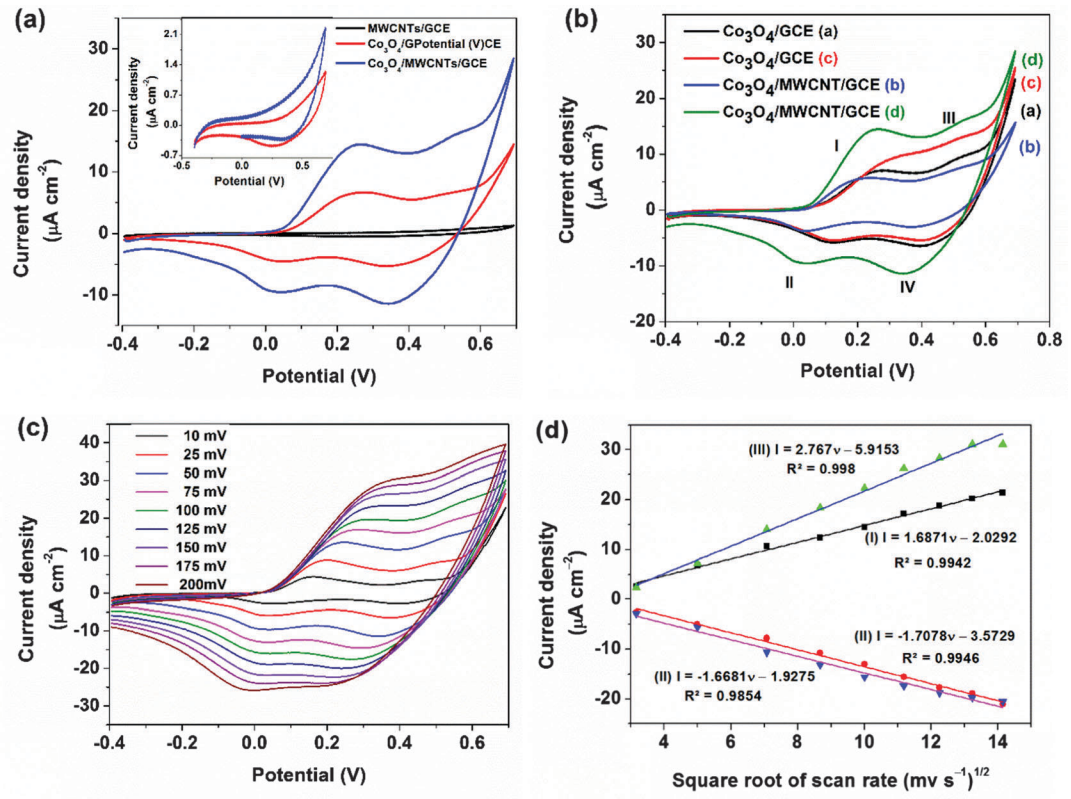

Fig. 3 (a) Cyclic voltammograms of Co_3O_4/GCE and Co_3O_4/MWCNT/GCE in 0.2 M NaOH and 0.1 M phosphate buffer solution (inset (a)), (b) cyclic voltammograms of Co_3O_4/GCE and Co_3O_4/MWCNT/GCE in the absence (a and b) and presence, (c and d) of 2.0 mM glucose in 0.2 M NaOH. Scan rate: 50 mV s^{-1}, (c) cyclic voltammograms of Co_3O_4/MWCNT/GCE at different scan rates from 10 mV s^{-1} to 200 mV s^{-1} in 0.2 M NaOH with 2.0 mM glucose and (d) plot of peak current density *vs.* square root of the scan rate.

 This journal is © The Royal Society of Chemistry and the Centre National de la Recherche Scientifique 2015

Published on 14 October 2015. Downloaded by Michigan State University on 19/01/2016 18:25:29.

This increase in current with increased glucose concentration is attributed to the direct catalytic activity of the Co_3O_4/MWCNT toward glucose. In addition, peak iii ($CoOOH \rightarrow CoO_2$) which causes the electro-oxidation of glucose is mainly mediated in a NaOH solution, hence the peak iii potential was applied for subsequent amperometric detection. It is also well known that glucose can be oxidized to produce gluconolactone through 2-electron electrochemical reaction.[19] Therefore the possible mechanism of glucose electrochemical oxidation reaction catalyzed by Co_3O_4 at peak iii (+0.55 V) can be illustrated as following in eqn (3).

$$2CoO_2 + C_6H_{12}O_6 \text{ (glucose)} \rightarrow 2CoOOH + C_6H_{10}O_6 \text{ (gluconolactone)} \quad (3)$$

The information about the electrochemical mechanism can be obtained from the relation between the peak current and scan rate potential. Hence the effect of the scan rate of electro-oxidation of glucose on the Co_3O_4/MWCNT/GCE was also investigated. Fig. 3c shows the cyclic voltammograms of the Co_3O_4/MWCNT/GCE with 2 mM glucose at different scan rates ranging from 10 to 200 mV s^{-1}. From the obtained results it is observed that the anodic and cathodic peak currents increased with increasing scan rate. From Fig. 3d the anodic and cathodic peak currents are linearly correlated to the square root of the scan rate $(mV\ s^{-1})^{1/2}$ and the corresponding linear regression equations with the linear correlation coefficient values are as follows

(i) $I_{pa}\ (A) = 1.6871\nu - 2.099\ (mV\ s^{-1})^{1/2}$, $(R^2 = 0.9942)$, (ii) $I_{pc}\ (A) = -1.7078\nu - 3.572\ (mV\ s^{-1})^{1/2}$, $(R^2 = 0.9946)$, (iii) $I_{pa}\ (A) = 2.767\nu - 5.9153\ (mV\ s^{-1})^{1/2}$, $(R^2 = 0.998)$ and (iv) $I_{pc}\ (A) = -1.6681\nu - 1.9275\ (mV\ s^{-1})^{1/2}$, $(R^2 = 0.9954)$.

Hence, these results indicate that the electrochemical kinetics is diffusion-controlled and it can also be ideal for quantitative analysis in practical applications. The CV was recorded for different glucose concentrations at 50 mV s^{-1} in 0.2 M NaOH solution (Fig. S3, ESI†). The studies show that the synergistic effect of Co_3O_4 NPs and the MWCNTs effectively electrocatalysed the direct glucose oxidation.

Since cyclic voltammetry has limitations for low concentration measurements, chronoamperometry responses were investigated to detect glucose. The chronoamperometry was executed by the successive addition of 50 μM glucose into 10 mL of 0.2 M NaOH solution at constant intervals. To investigate the best optimal applied potential, chronoamperometry was carried out at different applied potentials such as 0.5, 0.55 and 0.6 V to yield excellent electrochemical properties (Fig. 4a). From these results, it is seen that the signal-to-background ratio

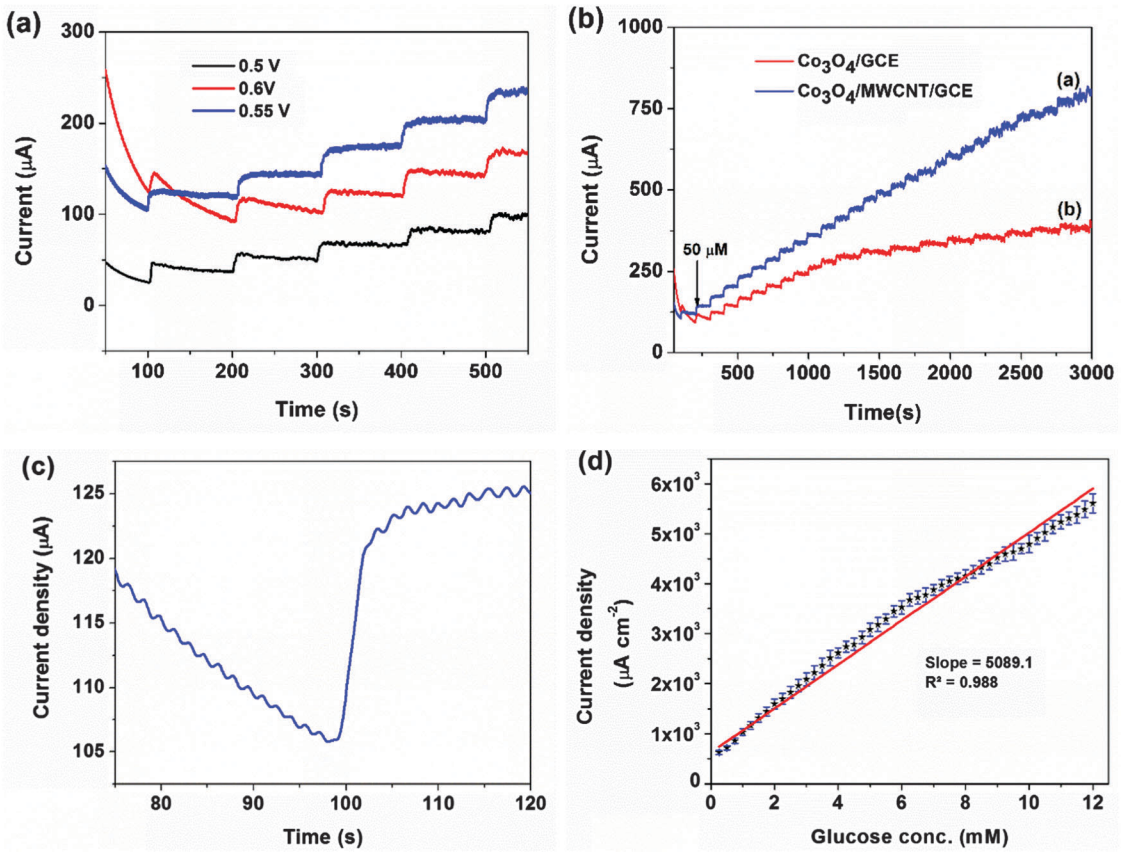

Fig. 4 (a) Amperometric responses of Co_3O_4/MWCNT/GCE at different potentials in 0.2 M NaOH with a dropwise addition of 50 μM glucose every 50 s, (b) current–time responses at 0.55 V with an increasing glucose concentration (50 μM) per 100 s for Co_3O_4/MWCNT/GCE, (c) response time measurement using the i–t curve and (d) the current density response *vs.* glucose concentration at the Co_3O_4/MWCNT/GCE.

Published on 14 October 2015. Downloaded by Michigan State University on 19/01/2016 18:25:29.

Table 1 Comparison of non-enzymatic glucose sensing performance based on different electrode materials of transition metal compounds

Electrode	Sensitivity ($\mu A\ mM^{-1}\ cm^{-2}$)	Linear range (up to, mM)	LOD (μM)	Applied potential (V)	Response time (s)	Ref.
Co_3O_4 nanofibers	36.25	2.04	0.97	+0.60	7	19
CuO nanospheres	404.53	2.6	1.0	+0.60	—	41
Ni NPs–CNF paste electrode	420.4	2.5	1.0	+0.55	5	42
CuO nanofibers	431.3	2.5	0.8	+0.40	1	43
SA-CNT thin films with Cu NPs electrode	602.0	1.8	0.1	+0.60	—	34
Ni nanowire arrays (NiNWAs)	1043	7.0	0.1	+0.55	—	44
CuxO flowers	1620	6.0	49	+0.50	—	45
CuO–MWCNTs array electrode	2190	3.0	0.8	+0.55	2	46
IrO_2/PbO_2-carbon microelectrodes	—	20	50	+0.75	0.5	47
Self-assembled Co_3O_4–MWCNT/GCE	**5089.1**	**12**	**10.42**	**+0.55**	**3**	Present work

increases with the potential range from 0.5 to 0.6 V and it is observed that the current response recorded for 0.55 V is greater than the other applied potentials which is supported by the CV results, where the glucose oxidation peak potential of ~0.55 V was observed. Hence, 0.55 V was chosen as an optimal applied potential for further chronoamperometry investigation. Under these optimal conditions, the chronoamperometry of the modified GCEs was examined. From Fig. 4b it can be seen that the current response recorded for the Co_3O_4/MWCNT/GCE (curve a) is 40% greater than the Co_3O_4/GCE (curve b) with the incremental addition of glucose (50 μM) and reaches 95% of the steady-state current within 5 s (Fig. 4c) indicating that the Co_3O_4/MWCNT nanocomposites efficiently catalyse the oxidation of glucose. The calibration curve for the electrochemical responses of the Co_3O_4/MWCNT/GCE to glucose concentration is shown in Fig. 4d. From the slope of the calibration curve, the sensitivity of the sensor was found to be 5089.1 $\mu A\ mM^{-1}\ cm^{-2}$ for a linear glucose concentration range from 0.05 mM to 12 mM with a linear coefficient of R^2 = 0.988. The limit of detection (LOD) is determined using eqn (4) and (5).

$$\text{Sensitivity} = \text{slope of the calibration curve} \quad (4)$$

$$\text{LOD} = \frac{3.3 \times \sigma}{\text{slope}} \quad (5)$$

where σ is the standard deviation of the slope. From the calculations, the LOD of the sensor was found to be 10.42 μM. The sensors were also compared with the previously reported nanomaterial based enzyme-free glucose sensors and are as shown in Table 1. As it can be seen from the table, the fabricated sensor shows highly enhanced sensitivity and LOD due to the excellent catalytic activity of Co_3O_4-NPs and the electrical network formed through self-assembled Co_3O_4-NPs distributing on the surface of the MWCNTs, which not only can keep their intrinsic excellent electrical conductivity but also facilitate easy access of Co_3O_4 NPs to glucose oxidation. Therefore, the direct electrochemical glucose oxidation can be greatly enhanced with the use of Co_3O_4/MWCNT composites.

Effects of interfering species, stability and reproducibility

Biomolecules like fructose, sucrose, maltose, AA, DA and UA are potentially interfering ions with human blood glucose and these may also get easily oxidized at the applied potential on the sensor electrode. Hence these interfering biomolecules were also tested amperometrically at +0.55 V along with glucose on the Co_3O_4/MWCNT/GCE in 0.2 M NaOH solution (Fig. 5). From Fig. 5 it can be seen that the response obtained for a 2 mM concentration of fructose, maltose, sucrose, AA, DA and UA was less than 3% of that obtained for 2 mM glucose which indicates the remarkable selectivity of the sensor for glucose detection in the presence of common interfering electroactive molecules.

Long term stability experiments were investigated to evaluate the performance of the Co_3O_4/MWCNT/GCE enzyme-free sensor, as shown in Fig. 6a. The sensor shows a current response to glucose over a period of three weeks (five identical electrodes) during which 85% current retained was observed. However, when the sensor was not in use it was stored in the lab atmosphere. These results suggest that the Co_3O_4/MWCNT/GCE possessed a good stability. The reproducibility was examined for ten identically constructed electrodes at 50 μM of glucose concentration, which shows a 4.1% relative standard deviation (RSD) suggesting excellent reproducibility (Fig. 6b). From these results, it may be confirmed that the Co_3O_4/MWCNT/GCE has a greater stability and reproducibility that makes it applicable for practical use.

Finally, as a real application, the Co_3O_4/MWCNT/GCE was applied for the determination of the glucose concentration in

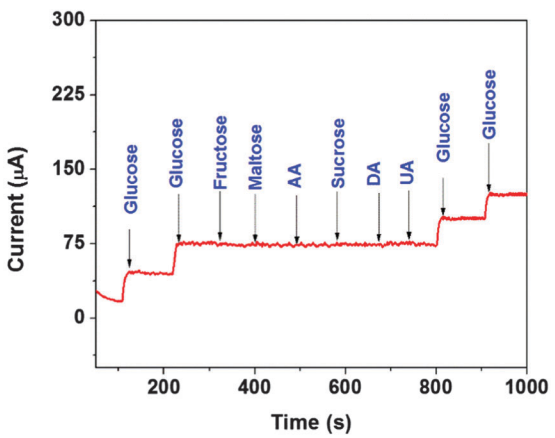

Fig. 5 Interference test of the sensor in 0.2 M NaOH at +0.55 V with 2 mM glucose and other interferons as indicated.

 This journal is © The Royal Society of Chemistry and the Centre National de la Recherche Scientifique 2015

Published on 14 October 2015. Downloaded by Michigan State University on 19/01/2016 18:25:29.

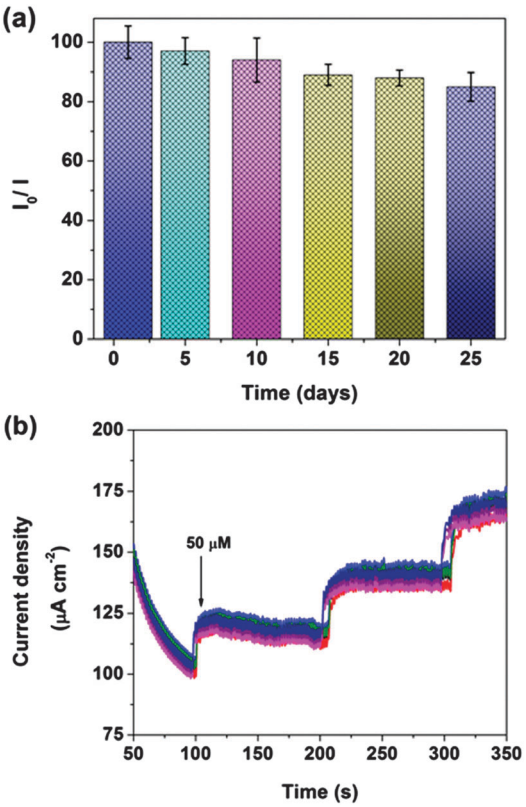

Fig. 6 (a) Stability of the sensor stored under ambient conditions over three weeks using 0.2 M NaOH with 2.0 mM glucose at +0.55 V and (b) *i*–*t* response for stability check using ten identical Co_3O_4/MWCNT/GC electrodes.

Table 2 The detection of glucose in human blood plasma samples

Sample	Glucose (mM)	RSD (N = 5) (%)	Glucose (mM) (commercial glucose meter)	Recovery (%)
1	6.1	4.4	6.3	96.4
2	4.6	3.8	4.9	94.2
3	4.5	5.2	4.6	96.4
4	5.1	3.7	5.2	97.6

human blood plasma samples. Blood plasma samples without any pre-treatments were injected into 5 mL of 0.2 M NaOH at an applied potential of +0.55 V. The measured current change was correlated with the glucose concentration according to the calibration curve in Fig. 4d and then compared with the value obtained using a commercial glucose meter (Free Style Freedom Lite Glucose Monitoring System, Abbott Diabetes Care) as shown in Table 2. The results show that the recovery of the samples is >94% with the relative standard deviation (RSD) less than 7%. Hence, these results suggest that the Co_3O_4/MWCNT/GCE composite is a potential material for the fabrication of enzyme-free glucose sensors.

Conclusions

Self-assembled uniformly decorated cobalt oxide nanoparticle decorated multi-walled carbon nanotubes were successfully synthesized by a simple wet chemical sol–gel method. The synthesized composite was employed to fabricate an enzyme-free glucose sensor for the detection of glucose. The results of cyclic voltammetry and chronoamperometry revealed that uniformly dispersed cobalt oxide on multi-walled carbon nanotubes possessed attractive electrochemical properties such as high sensitivity, low detection limit, high selectivity, greater stability and excellent reproducibility. These improved performances are ascribed to the synergistic effect of cobalt oxide and multi-walled carbon nanotubes. Thus, the cobalt oxide-multi-walled carbon nanotube nanocomposites are expected to be promising materials for the fabrication of enzyme-free glucose sensors.

Acknowledgements

The authors are thankful to CeNSE, Indian Institute of Science, Bangalore for providing analytical services and NITK, Surathkal, India, for providing necessary laboratory facilities.

References

1 J. Wang, *Electroanalysis*, 2005, **17**, 7–14.
2 H. Jiang, *Small*, 2011, **7**, 2413–2427.
3 M. Gao, L. Dai and G. G. Wallace, *Electroanalysis*, 2003, **15**, 1089–1094.
4 T. Zhu, B. Xia, L. Zhou and X. W. (David) Lou, *J. Mater. Chem.*, 2012, **22**, 7851–7855.
5 Z. Dong, C. Zhou, H. Cheng, Y. Zhao, C. Hu, N. Chen, Z. Zhang, H. Luo and L. Qu, *Carbon*, 2013, **64**, 507–515.
6 N. G. Tsierkezos, U. Ritter, N. Wetzold and A. C. Hübler, *Microchim. Acta*, 2012, **179**, 157–161.
7 C. Lu, W. Liu, H. Li and B. K. Tay, *Chem. Commun.*, 2014, **50**, 3338–3340.
8 P. H. Jampani, O. Velikokhatnyi, K. Kadakia, D. H. Hong, S. S. Damle, J. A. Poston, A. Manivannan and P. N. Kumta, *J. Mater. Chem. A*, 2015, **3**, 8413–8432.
9 R. Prasad, N. Gorjizadeh, R. Rajarao, V. Sahajwalla and B. R. Bhat, *RSC Adv.*, 2015, **5**, 44792–44799.
10 R. Prasad and B. R. Bhat, *Sens. Actuators, B*, 2015, **220**, 81–90.
11 F. Sun, L. Li, P. Liu and Y. Lian, *Electroanalysis*, 2011, **23**, 395–401.
12 H. Yu, X. Jian, J. Jin, X. Zheng, R. Liu and G. Qi, *Microchim. Acta*, 2014, **182**, 157–165.
13 X.-C. Dong, H. Xu, X.-W. Wang, Y.-X. Huang, M. B. Chan-Park, H. Zhang, L.-H. Wang, W. Huang and P. Chen, *ACS Nano*, 2012, **6**, 3206–3213.
14 X. Wang, X. Dong, Y. Wen, C. Li, Q. Xiong and P. Chen, *Chem. Commun.*, 2012, **48**, 6490–6492.
15 L. Zhang, S. Yuan, L. Yang, Z. Fang and G. Zhao, *Microchim. Acta*, 2013, **180**, 627–633.
16 J. Yuan, Y. Cen, X.-J. Kong, S. Wu, C.-L. Liu, R.-Q. Yu and X. Chu, *ACS Appl. Mater. Interfaces*, 2015, **7**(19), 10548–10555.
17 J. Lang, X. Yan and Q. Xue, *J. Power Sources*, 2011, **196**, 7841–7846.

Published on 14 October 2015. Downloaded by Michigan State University on 19/01/2016 18:25:29.

18 S. G. Kandalkar, J. L. Gunjakar and C. D. Lokhande, *Appl. Surf. Sci.*, 2008, **254**, 5540–5544.
19 Y. Ding, Y. Wang, L. Su, M. Bellagamba, H. Zhang and Y. Lei, *Biosens. Bioelectron.*, 2010, **26**, 542–548.
20 C.-W. Kung, C.-Y. Lin, Y.-H. Lai, R. Vittal and K.-C. Ho, *Biosens. Bioelectron.*, 2011, **27**, 125–131.
21 S. Yang, G. Cui, S. Pang, Q. Cao, U. Kolb, X. Feng, J. Maier and K. Müllen, *ChemSusChem*, 2010, **3**, 236–239.
22 W. Y. Li, L. N. Xu and J. Chen, *Adv. Funct. Mater.*, 2005, **15**, 851–857.
23 Z. Meng, B. Liu, J. Zheng, Q. Sheng and H. Zhang, *Microchim. Acta*, 2011, **175**, 251–257.
24 G. Wang, X. Shen, J. Yao, D. Wexler and J. Ahn, *Electrochem. Commun.*, 2009, **11**, 546–549.
25 A. Tavasoli, K. Sadagiani, F. Khorashe, A. A. Seifkordi, A. A. Rohani and A. Nakhaeipour, *Fuel Process. Technol.*, 2008, **89**, 491–498.
26 L. Fu, Z. Liu, Y. Liu, B. Han, P. Hu, L. Cao and D. Zhu, *Adv. Mater.*, 2005, **17**, 217–221.
27 A. Heller and B. Feldman, *Chem. Rev.*, 2008, **108**, 2482–2505.
28 D. Chirizzi, M. R. Guascito, C. Malitesta and E. Mazzotta, in *Sensors and Microsystem*, ed. G. Neri, N. Donato, A. d'Amico and C. D. Natale, Springer, Netherlands, 2011, pp. 339–343.
29 A. Badia, R. Carlini, A. Fernandez, F. Battaglini, S. R. Mikkelsen and A. M. English, *J. Am. Chem. Soc.*, 1993, **115**, 7053–7060.
30 C. Malitesta, F. Palmisano, L. Torsi and P. G. Zambonin, *Anal. Chem.*, 1990, **62**, 2735–2740.
31 M. Wooten, S. Karra, M. Zhang and W. Gorski, *Anal. Chem.*, 2014, **86**, 752–757.
32 R. Wilson and A. P. F. Turner, *Biosens. Bioelectron.*, 1992, **7**, 165–185.
33 X. Kang, Z. Mai, X. Zou, P. Cai and J. Mo, *Anal. Biochem.*, 2007, **363**, 143–150.
34 X. Li, Q. Zhu, S. Tong, W. Wang and W. Song, *Sens. Actuators, B*, 2009, **136**, 444–450.
35 Z. H. Ibupoto, K. Khun, V. Beni, X. Liu and M. Willander, *Sensors*, 2013, **13**, 7926–7938.
36 S. Park, H. Boo and T. D. Chung, *Anal. Chim. Acta*, 2006, **556**, 46–57.
37 R. Rajarao and B. R. Bhat, *Synth. React. Inorg., Met.-Org., Nano-Met. Chem.*, 2013, **43**, 1418–1422.
38 J. Wu, Y. Xue, X. Yan, W. Yan, Q. Cheng and Y. Xie, *Nano Res.*, 2012, **5**, 521–530.
39 D. Jung, M. Han and G. S. Lee, *Sens. Actuators, B*, 2014, **204**, 596–601.
40 N. Yan, L. Hu, Y. Li, Y. Wang, H. Zhong, X. Hu, X. Kong and Q. Chen, *J. Phys. Chem. C*, 2012, **116**, 7227–7235.
41 E. Reitz, W. Jia, M. Gentile, Y. Wang and Y. Lei, *Electroanalysis*, 2008, **20**, 2482–2486.
42 Y. Liu, H. Teng, H. Hou and T. You, *Biosens. Bioelectron.*, 2009, **24**, 3329–3334.
43 W. Wang, L. Zhang, S. Tong, X. Li and W. Song, *Biosens. Bioelectron.*, 2009, **25**, 708–714.
44 L.-M. Lu, L. Zhang, F.-L. Qu, H.-X. Lu, X.-B. Zhang, Z.-S. Wu, S.-Y. Huan, Q.-A. Wang, G.-L. Shen and R.-Q. Yu, *Biosens. Bioelectron.*, 2009, **25**, 218–223.
45 C. Li, Y. Su, S. Zhang, X. Lv, H. Xia and Y. Wang, *Biosens. Bioelectron.*, 2010, **26**, 903–907.
46 J. Yang, L.-C. Jiang, W.-D. Zhang and S. Gunasekaran, *Talanta*, 2010, **82**, 25–33.
47 W. Gorski and R. T. Kennedy, *J. Electroanal. Chem.*, 1997, **424**, 43–48.

 This journal is © The Royal Society of Chemistry and the Centre National de la Recherche Scientifique 2015